Localizing the Shape Transition in Neutron-Deficient Selenium

J. Henderson, C. Y. Wu, J. Ash, P. C. Bender, B. Elman, A. Gade, M. Grinder, H. Iwasaki, E. Kwan, B. Longfellow, T. Mijatović, D. Rhodes, M. Spieker, and D. Weisshaar

Phys. Rev. Lett. **121**, 082502 — Published 22 August 2018

DOI: 10.1103/PhysRevLett.121.082502

Localizing the shape transition in neutron-deficient selenium

J. Henderson,[1,*] C. Y. Wu,[1] J. Ash,[2,3] P. C. Bender,[4] B. Elman,[2,3] A. Gade,[2,3] M. Grinder,[2,3] H. Iwasaki,[2,3] E. Kwan,[2] B. Longfellow,[2,3] T. Mijatović,[2] D. Rhodes,[2,3] M. Spieker,[2] and D. Weisshaar[2]

[1]*Lawrence Livermore National Laboratory, Livermore, CA 94550, USA*
[2]*National Superconducting Cyclotron Laboratory, Michigan State University, East Lansing, MI 48824, USA*
[3]*Department of Physics and Astronomy, Michigan State University, East Lansing, MI 48824, USA*
[4]*Department of Physics and Applied Physics, University of Massachusetts Lowell, Lowell, MA 01854, USA*

(Dated: July 23, 2018)

Neutron-deficient selenium isotopes are thought to undergo a rapid shape change from a prolate deformation near the line of beta-stability towards oblate deformation around the line of $N = Z$. The point at which this shape change occurs is unknown, with inconsistent predictions from available theoretical models. A common feature in the models is the delicate nature of the point of transition, with the introduction of even a modest spin to the system sufficient to change the ordering of the prolate and oblate configurations. We present a measurement of the quadrupole moment of the first-excited state in radioactive ^{72}Se - a potential point of transition - by safe Coulomb excitation. This is the first low-energy Coulomb excitation to be performed with a rare-isotope beam at the reaccelerated beam facility (ReA3) at the National Superconducting Cyclotron Laboratory (NSCL). By demonstrating a negative spectroscopic quadrupole moment for the first-excited 2^+ state, it is found that any low-spin shape change in neutron-deficient selenium does not occur until ^{70}Se.

Nuclei rapidly develop degrees of quadrupole deformation as proton and neutron numbers deviate from the so-called "magic numbers" which enforce spherical shapes at low energy. In certain cases, nuclei exhibit multiple structures with different deformation at comparable excitation energy, giving rise to the phenomenon of shape coexistence (see Ref. [1] and references therein). Often this coexistence is manifest across a range of nuclei in an isotopic chain, with the total energies of different prolate or oblate configurations changing rather dramatically with the addition or removal of only a pair of neutrons. The consequence of this is that the deformation of the lowest-lying configuration undergoes a rapid change between isotopes differing by only two nucleons.

Neutron-deficient selenium isotopes are thought to make up a region of the nuclear landscape wherein such a sudden shape change occurs. Selenium nuclei in the vicinity of the line of β-stability exhibit prolate deformation, corroborated by polarized inelastic proton scattering measurements [2, 3] and the observation of negative spectroscopic quadrupole moments [4–7]. Under the assumptions of axial symmetry and strong coupling, and with the nuclear spin aligned with the axis of rotation, these negative spectroscopic quadrupole moments correspond to a prolate deformation. Away from stability, a measurement of the kinetic moments of inertia of ^{68}Se indicates a strong preference for oblate deformation at low spin [8], pointing towards a shape transition occurring beyond the most neutron-deficient stable selenium isotope (^{74}Se). Kinetic moments of inertia also indicate an oblate deformation for low-lying states in ^{70}Se [8]. A Coulomb-excitation measurement of the spectroscopic quadrupole moment of the first-excited 2_1^+ state, $Q_s(2_1^+)$, in ^{70}Se was initially in conflict with this picture, pointing towards a prolate deformation [9], however a subsequent re-evaluation after an improved measurement of the 2_1^+ state lifetime eventually demonstrated a preference for an oblate deformation [10].

Measurements therefore indicate that a shape transition occurs between prolate ^{74}Se and oblate ^{68,70}Se, however whether this shape change takes place at ^{70}Se or ^{72}Se is unclear. Theoretical calculations differ in their predictions of the point of shape change. A comparison of available experimental data with the interacting boson model with configuration mixing (IBM-CM) did show a preference for low-lying oblate deformation in ^{72}Se [11]. A number of calculations using mean-field methodologies have been performed and variously predict an oblate shape for low-spin states ^{72}Se [12], or a prolate configuration in ^{72}Se [13, 14], with oblate configurations only becoming dominant in the ground-state in ^{70}Se. Shell-model calculations [15] predict oblate low-spin states in ^{72}Se, with the prolate structure becoming yrast at higher spin. Common to all calculations is the delicacy of the shape minimum, with the introduction of even modest spin to the system being sufficient to alter the ordering of the configurations in favor of prolate deformation.

In order to establish the deformation of ^{72}Se, safe Coulomb excitation was employed in the first rare-isotope-beam low-energy Coulomb excitation experiment performed at the reaccelerated beam facility (ReA3 [16]) of the National Superconducting Cylotron Laboratory (NSCL [17]). The secondary beam of ^{72}Se was produced from the fragmentation of a 150 MeV/u ^{78}Kr primary beam and selected in the A1900 fragment separator [18]. The ^{72}Se ions were transported to the linear gas stopper, thermalized, and extracted before charge breeding to Q=17$^+$ in NSCL's electron beam ion trap [19]. The charge-bred ions were then injected into the ReA3 accelerator chain and accelerated to an energy of 4.0 MeV/u.

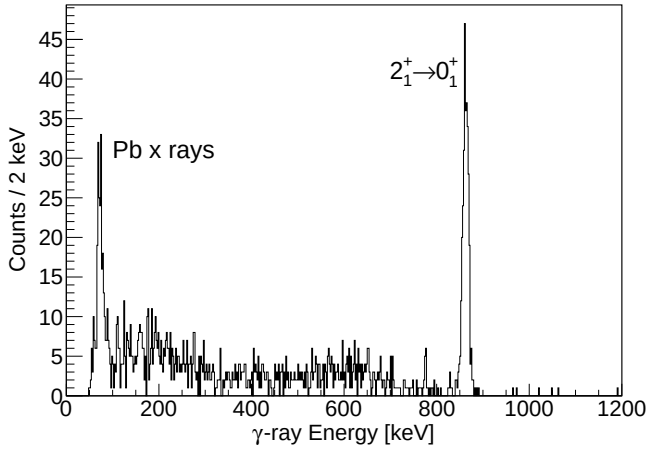

FIG. 1. Doppler-corrected γ rays coincident with the detection of scattered ^{72}Se in the downstream silicon detector. The 862-keV $2_1^+ \rightarrow 0_1^+$ transition is clearly visible. Observation of the $0_2^+ \rightarrow 2_1^+$ transition at 75 keV was prevented by the large yield of lead x rays at a similar energy.

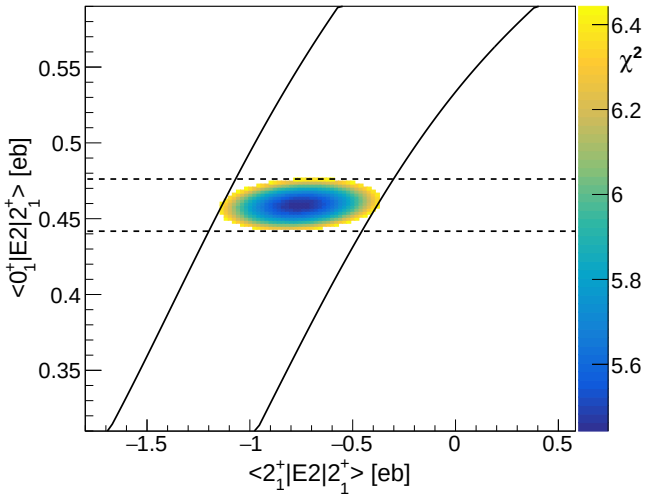

FIG. 2. The 1σ limit, corresponding to values between χ^2_{min} and $\chi^2_{min} + 1$ of the χ^2 surface arising from the fitting of GOSIA calculations to experimental data and literature $B(E2; 2_1^+ \rightarrow 0_1^+)$ while varying $\langle 0_1^+ | E2 | 2_1^+ \rangle$ and $\langle 2_1^+ | E2 | 2_1^+ \rangle$. Dashed lines correspond to the evaluated literature uncertainty on $\langle 0_1^+ | E2 | 2_1^+ \rangle$ from lifetime measurements [24]. The solid lines demark the statistical 1σ uncertainty band reached without including the literature $B(E2; 2_1^+ \rightarrow 0_1^+)$ in the determination of the χ^2.

Accelerated ^{72}Se ions were impinged upon an enriched, 0.92-mg/cm^2 thick ^{208}Pb target with a 50 μg/cm^2 carbon backing at typical on-target intensities of 4000 pps over a period of 90 hours. The target was located within the JANUS setup for Coulomb excitation [20], consisting of a pair of S3-type annular silicon detectors located upstream and downstream of the target. The downstream and upstream target-silicon detector separations were measured to be 26 ± 1 mm and 34 ± 1 mm, respectively. The choice of beam energy was such that the distance of closest approach of the beam and target nuclei was never less than 6 fm, ensuring an electromagnetic excitation. De-exciting γ rays were detected in the Segmented Germanium Array (SeGA) [21], consisting of 16 32-fold segmented HPGe detectors. Data were extracted using a digital data-acquisition system, made up of 33 100-MHz (SeGA) and 8 250-MHz (silicon detectors) XIA Pixie-16 modules in a triggerless, continuous-running mode, with events constructed on the basis of a master clock and analyzed using the GRUTinizer [22] software package, built in a ROOT framework [23].

The kinematics of the reaction are such that both beam (^{72}Se) and target (^{208}Pb) nuclei scattered into the downstream silicon detector, corresponding to different angular ranges in the center-of-mass frame. Beam and target nuclei were selected by their observed kinematics in the silicon detectors. Gamma rays were Doppler corrected on the basis of the ^{72}Se kinematics, determined from the measured scattering angle of the observed beam or target nuclei. Figure 1 shows the Doppler-corrected γ-ray spectrum determined from the detection of the ^{72}Se nuclei. A γ ray corresponding to the 862-keV $2_1^+ \rightarrow 0_1^+$ transition is clearly seen. No other transitions could be unambiguously identified above background, with the $0_2^+ \rightarrow 2_1^+$

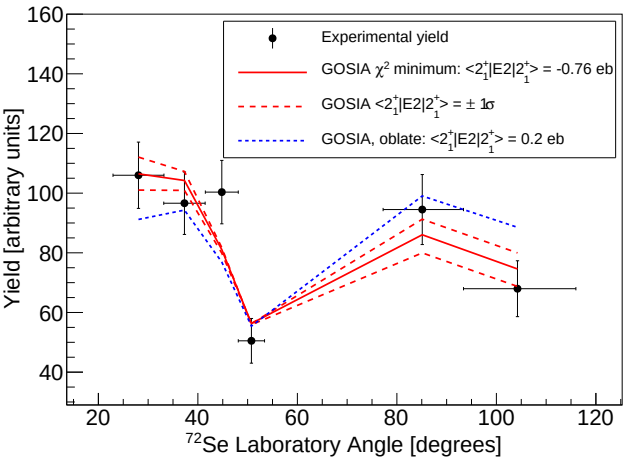

FIG. 3. Experimental Coulomb excitation yields (points) vs laboratory scattering angle of ^{72}Se. Also shown are the calculated yields (see text for details) corresponding to the best fit to the experimental data, along with the $\pm 1\sigma$ limits on $\langle 2_1^+ | E2 | 2_1^+ \rangle$, with scaling as described in the text. Horizontal error bars are representative of the angular range and do not correspond to an uncertainty. For comparison, calculated yields for an oblate deformation with $\langle 2_1^+ | E2 | 2_1^+ \rangle = 0.2$ eb are shown, corresponding to the approximate oblate deformation thought to occur in ^{70}Se [12–14].

TABLE I. Reduced matrix elements from literature between initial (I) and final (F) states used to constrain the present result. Uncertainties are quoted at $\pm 1\sigma$. Note that the $\langle 0_1^+ | E2 | 2_1^+ \rangle$ matrix element was varied in order to create the χ^2 surface seen in Fig. 2. See text for details.

	$\langle I \vert E2 \vert F \rangle$ [eb]	Reference
$\langle 0_1^+ \vert E2 \vert 2_1^+ \rangle$	0.459 ± 0.017	[24]
$\langle 0_1^+ \vert E2 \vert 2_2^+ \rangle$	$0.065^{+0.003}_{-0.005}$	[11]
$\langle 2_1^+ \vert E2 \vert 0_2^+ \rangle$	$0.532^{+0.035}_{-0.037}$	[11]
$\langle 2_1^+ \vert E2 \vert 2_2^+ \rangle$	$0.817^{+0.028}_{-0.054}$	[11]
$\langle 2_1^+ \vert E2 \vert 4_1^+ \rangle$	$0.939^{+0.044}_{-0.085}$	[11]
$\langle 0_2^+ \vert E2 \vert 2_2^+ \rangle$	$0.566^{+0.047}_{-0.024}$	[11]
	$\langle I \vert M1 \vert F \rangle$ [μ_n]	Reference
$\langle 2_1^+ \vert M1 \vert 2_2^+ \rangle$	$0.029^{+0.001}_{-0.002}$	[11]

transition indistinguishable from lead x rays originating from the target.

The use of a ^{208}Pb target provides an exceptionally clean γ-ray spectrum, but precludes the normalization of the observed beam excitation yields to that of the target due to the lack of significant population of states in the target nucleus. Instead, sensitivity to the quadrupole moment of the ^{72}Se 2_1^+ state was achieved through the angular distribution of the cross section by the so-called reorientation effect [25]. Nuclei with non-spherical charge distributions undergo reorientation in the presence of the large electric field gradient of the target nuclei, inducing a second-order angular dependence to the cross section. For certain kinematic solutions, threshold effects arising from silicon dead layers resulted in reductions in the observed intensity and therefore an additional angular dependence to the measured cross section. This cannot be disentangled from the reorientation effect and therefore yields coincident with detection of ^{208}Pb at lab angles greater than 42° were excluded, as well as detections of ^{72}Se in the upstream silicon detector. The integrity of the remaining data was confirmed through comparison of the silicon-singles data with the expected angular distribution of the Rutherford cross section, which was also employed to confirm the target-detector separation. Measured yields were then corrected for efficiency and separated into six angular bins: four corresponding to the detection of ^{72}Se and two to the detection of ^{208}Pb, corresponding to center-of-mass angles of $31° \rightarrow 69°$ and $97° \rightarrow 133°$, respectively.

The diagonal matrix element $\langle 2_1^+ | E2 | 2_1^+ \rangle$, and thus the spectroscopic quadrupole moment of the 2_1^+ state, was extracted through comparison with yields calculated with the GOSIA Coulomb-excitation code [26]. Integrated yields were calculated in GOSIA for the experimental conditions presented. Matrix elements for non-observed transitions were included from Refs. [11] and [24], and are shown in Table I. A single parameter was then used to scale the calculated yields in order to best fit the experimental data for each given matrix element combination. A χ^2 surface was created by varying the $\langle 0_1^+ | E2 | 2_1^+ \rangle$ and $\langle 2_1^+ | E2 | 2_1^+ \rangle$ matrix elements used to calculate the yields. This method allowed for corrections due to an $E0$ component to the decay of the 0_2^+ state, the systematic effects of which are discussed below. Due to the scaling applied and the absence of normalization, there was no strong sensitivity to the $\langle 0_1^+ | E2 | 2_1^+ \rangle$ matrix element. A correlation between the two varied matrix elements was observed and the literature $B(E2; 2_1^+ \rightarrow 0_1^+)$ was therefore incorporated into the χ^2 surface in order to localize $\langle 2_1^+ | E2 | 2_1^+ \rangle$. The 1σ χ^2 surface is shown in Fig. 2, along with lines demarking the 1σ limits on $\langle 2_1^+ | E2 | 2_1^+ \rangle$ for a range of $\langle 0_1^+ | E2 | 2_1^+ \rangle$. The present data indicate a prolate deformation at a better than 1σ level. Figure 3 shows the measured experimental yields, along with those calculated in GOSIA corresponding to the minimized χ^2 and the 1σ limits for the $\langle 2_1^+ | E2 | 2_1^+ \rangle$ matrix element. Also shown for comparison is the yield distribution expected for an oblate deformation with a quadrupole moment approximately equivalent to that expected in ^{70}Se [10, 13, 14].

Systematic uncertainties arising from variations in the matrix elements of non-observed transitions were investigated by varying them to the literature $\pm 1\sigma$ limits and repeating the minimization procedure. Similarly, the systematic uncertainty due to the uncertainty in the target to silicon detector separation was investigated by repeating the minimization procedure at the $\pm 1\sigma$ limits. Based on the transition matrix elements in Table I the excited 0_2^+ state at 937 keV in ^{72}Se is expected to be populated, and has been found to decay [27] by both an $E2$ transition to the 2_1^+ state and by an $E0$ transition to the ground state by the emission of a conversion electron. Because GOSIA does not explicitly allow for state de-excitation by $E0$ transitions, the calculated yields were corrected according to the literature branching ratio for this state. This uncertainty was again determined by varying the branching ratio to the literature $\pm 1\sigma$ levels. Based on these considerations, and the aforementioned minimization procedure, we extract $\langle 2_1^+ | E2 | 2_1^+ \rangle = -0.76 \pm 0.38(\text{stat.}) \pm 0.14(\text{sys.})$ eb, corresponding to a spectroscopic quadrupole moment of $Q_s(2_1^+) = -0.57 \pm 0.29(\text{stat.}) \pm 0.10(\text{sys.})$ eb, thereby indicating a 2_1^+ state dominated by prolate configurations in ^{72}Se.

The present measurement yields a spectroscopic quadrupole moment consistent with those seen in heavier selenium isotopes, as shown in Fig. 4. This indicates that the well-deformed prolate structure found in ^{74,76}Se continues to dominate the low-lying configurations in selenium isotopes until ^{70}Se, at which point it is overcome by the coexisting oblate structure. We note that, while the result for ^{70}Se shows a preference for oblate deformation, it remains consistent with a modest prolate deformation within the 1σ limits, though inconsistent with a continu-

ation of the relatively constant spectroscopic quadrupole moment in heavier selenium isotopes. While the present measurement strongly indicates a prolate nature for the 2_1^+ state in ^{72}Se it lacks explicit sensitivity to the deformation of the ground state. Theoretical calculations in Refs. [10, 13–15] indicate that, even in the case of an oblate ground state, prolate configurations dominate at modest spin ($I(\hbar) \geq 4$). In the event that significant state mixing takes place with different wavefunction admixtures in the ground and first-excited states, the assumption of equal 0_1^+ and 2_1^+ state deformations may break down.

The non-zero measured electric-monopole transition strength, $\rho^2(E0; 0_2^+ \rightarrow 0_1^+) \cdot 10^3 = 31 \pm 4$ [11, 27] points towards a degree of mixing, however the significance of the mixing cannot be uniquely determined. In a ^{74}Se$(p,t)^{72}$Se study [28], the integrated cross-section to the 0_2^+ state in ^{72}Se was found to be 11% of that to the ground state, however no interpretation of the two-neutron transfer amplitude was provided. An evaluation of the observed (p,t) cross-section ratio using a distorted-wave Born approximation (DWBA) analysis was therefore performed with the PTOLEMY code [29] to account for any Q-value dependence. From this the extracted two-neutron transfer amplitude for the 0_2^+ state relative to the ground state was 9%. The evaluation was validated by comparing ^{76}Se$(p,t)^{74}$Se data from Ref. [28] with a more recent study [30]. This represents an enhancement over the same ratio for stable selenium isotopes, indicating some mixing between the 0_1^+ and 0_2^+ states, albeit with a ground state dominated by a configuration similar in nature to the prolate ground state found in ^{74}Se. The relative extracted two-neutron transfer amplitudes agree well with the prolate deformation inferred from the spectroscopic quadrupole moment of the present work. The 2_1^+ and 2_3^+ states have previously been assigned [31] as being built on the 0_1^+ and 0_2^+ band heads. The larger energy spacing between the 2^+ states implies a reduced mixing as compared to the 0^+ states, however this picture is complicated by the presence of the 2_2^+ state. In this interpretation the 2_2^+ state would be assigned as being the band-head of the so-called γ-band. The available data therefore indicate some mixing between the 0_1^+ and 0_2^+ states, but imply that it is relatively modest, with one dominant configuration and with no clear indication of increased mixing between 2^+ states. This indicates that the observed deformation in the present work dominates the ground-state configuration.

In order to complete our understanding of the low-lying states in ^{72}Se, a broader set of $E2$ matrix elements is required [34, 35], along with, for example $E0$ transition strengths between 2^+ states, providing further sensitivity to state mixing (see, e.g. Ref. [36]), or further two-neutron transfer experiments to determine shape evolution from ^{74}Se to ^{72}Se. Nonetheless, a number of theoretical approaches have been employed to determine $Q_s(2_1^+)$,

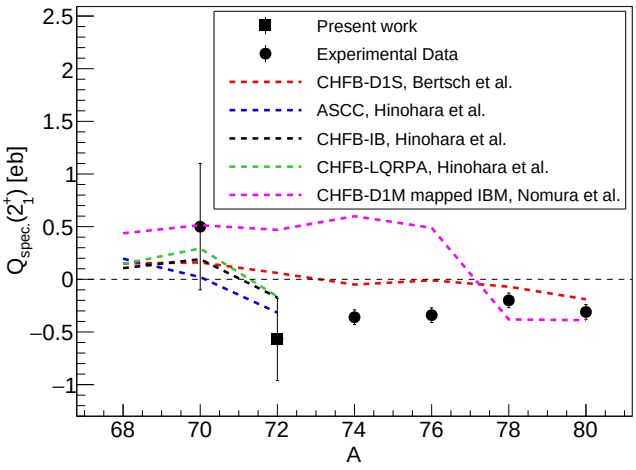

FIG. 4. Spectroscopic quadrupole moments for the first-excited 2^+ states in neutron-deficient selenium isotopes. Experimental data [10, 24] (points) are compared to theoretical calculations [12–14, 32]. Calculated values for the model described in Ref. [12] are tabulated in Ref. [33]. Note that the experimental data point for ^{70}Se is an approximation based on the data available in Ref. [10]. Here the uncertainty on the present measurement ($A = 72$) is the sum of the statistical and systematic uncertainties.

which will be discussed below. The relevant models are: a constrained Hartree-Fock-Bogliubov (CHFB), Gogny-D1M mapped interacting boson model (IBM) [32], a CHFB Gogny-D1S model described in Ref. [12] (tabulated in Ref. [33]), the adiabatic self-consistent collective coordinate (ASCC) method [13, 37] a CHFB method [14] using both a local quasiparticle random phase approximation (LQRPA) and Inglis-Balyaev (IB) defined normal modes, and a calculation based on the PMMU shell-model Hamiltonian [38]. All of these models are able to tackle the question of shape coexistence, however they use very different inputs. The PMMU shell-model Hamiltonian yields a positive $Q_s(2_1^+)$ [38], contradicting the present work, however the magnitude is not specified and as such it is not plotted in Fig. 4. The different behavior of the two Gogny-derived results [12, 32, 33] indicates that the collective nuclear motion may be treated rather differently in the five dimensional collective Hamiltonian (5DCH) [12] approach when compared to the IBM mapping approach used in Ref. [32]. The IBM-mapped results provide a better description of the absolute $Q_s(2_1^+)$ values and the suddenness of the transition, but fail to reproduce the exact point at which it occurs, while the Gogny-D1S approach fails to reproduce the absolute values. In contrast, the Gogny-D1S model [12] reproduces the evolution and absolute values of $Q_s(2_1^+)$ well in the krypton isotopes, which also exhibit shape coexistence. A possible explanation for this discrepancy is the increased γ-softness of the selenium isotopes, which may require a more delicate treatment than the relatively γ-rigid kryp-

ton. All three of the models described in Refs. [13, 14] use a pairing plus quadrupole (P+Q) interaction and produce approximately the same results, all in good agreement with experiment. The (β, γ) surfaces derived in these calculations indicate a highly γ-soft 0^+ ground state, with a 2_1^+ state dominated by prolate configurations and *yrast* states of higher spin being purely prolate. By comparison, the models of Refs. [13, 14] predict ^{68,70}Se to have ground and *yrast* states dominated by oblate configurations. Due to the apparent delicacy of the shape minima in the selenium isotopes, it would be of considerable interest to determine the sensitivity of the available models, with small changes in model parameters potentially being significant [39].

In summary, we present a low-energy Coulomb excitation measurement of ^{72}Se, the first such measurement with a rare-isotope beam to be performed at the NSCL ReA3 facility. The observed angular distribution of the 2_1^+ population cross section is consistent with a negative spectroscopic quadrupole moment at a better than 1σ level. Viewed in the context of a previous Coulomb excitation measurement [9, 10], this indicates that the anticipated transition from prolate to oblate shape in neutron-deficient selenium occurs between ^{72}Se and ^{70}Se. Furthermore, this measurement demonstrates the potential reach of Coulomb excitation with the reaccelerated beam program at both the NSCL and the Facility for Rare Isotope Beams (FRIB), with even relatively modest intensities of rare-isotope beams being sufficient to access spectroscopic quadrupole moments.

The authors thank the CCF, gas catcher and ReA3 beam delivery groups at the NSCL for the high-quality beam of ^{72}Se. Fruitful discussions with B. P. Kay and W. Nazarewicz are gratefully acknowledged. Work at LLNL was performed under contract DE-AC52-07NA27344. This work was supported in part by the National Science Foundation under Contract No. PHY-1565546 (NSCL), by the US Department of Energy, Office of Nuclear Physics, under Grant No. DE-FG02-08ER41556 (NSCL) and by the DOE National Nuclear Security Administration through the Nuclear Science and Security Consortium, under Award No. DE-NA0003180.

* henderson64@llnl.gov

[1] K. Heyde and J. L. Wood, Rev. Mod. Phys. **83**, 1467 (2011).
[2] S. Matsuki, T. Higo, T. Ohsawa, T. Shiba, T. Yanabu, K. Ogino, Y. Kadota, K. Haga, N. Sakamoto, K. Kume, and M. Matoba, Phys. Rev. Lett. **51**, 1741 (1983).
[3] W. H. L. Moonen, P. J. van Hall, S. S. Klein, G. J. Nijgh, C. W. A. M. van Overveld, R. M. A. L. Petit, and O. J. Poppema, Journal of Physics G **19**, 635 (1993).
[4] P. Raghavan, Atomic Data and Nuclear Data Tables **42**, 189 (1989).
[5] A. Kavka, C. Fahlander, A. Backlin, D. Cline, T. Czosnyka, R. Diamond, D. Disdier, W. Kernan, L. Kraus, I. Linck, N. Schulz, J. Srebrny, F. Stephens, L. Svensson, B. Varnestig, E. Vogt, and C. Wu, Nuclear Physics A **593**, 177 (1995).
[6] R. Lecomte, P. Paradis, J. Barrette, M. Barrette, G. Lamoureux, and S. Monaro, Nuclear Physics A **284**, 123 (1977).
[7] R. Lecomte, S. Landsberger, P. Paradis, and S. Monaro, Phys. Rev. C **18**, 2801 (1978).
[8] S. M. Fischer, C. J. Lister, and D. P. Balamuth, Phys. Rev. C **67**, 064318 (2003).
[9] A. M. Hurst, P. A. Butler, D. G. Jenkins, P. Delahaye, F. Wenander, F. Ames, C. J. Barton, T. Behrens, A. Bürger, J. Cederkäll, E. Clément, T. Czosnyka, T. Davinson, G. de Angelis, J. Eberth, A. Ekström, S. Franchoo, G. Georgiev, A. Görgen, R.-D. Herzberg, M. Huyse, O. Ivanov, J. Iwanicki, G. D. Jones, P. Kent, U. Köster, T. Kröll, R. Krücken, A. C. Larsen, M. Nespolo, M. Pantes, E. S. Paul, M. Petri, H. Scheit, T. Sieber, S. Siem, J. F. Smith, A. Steer, I. Stefanescu, N. U. H. Syed, J. Van de Walle, P. Van Duppen, R. Wadsworth, N. Warr, D. Weisshaar, and M. Zielińska, Phys. Rev. Lett. **98**, 072501 (2007).
[10] J. Ljungvall, A. Görgen, M. Girod, J.-P. Delaroche, A. Dewald, C. Dossat, E. Farnea, W. Korten, B. Melon, R. Menegazzo, A. Obertelli, R. Orlandi, P. Petkov, T. Pissulla, S. Siem, R. P. Singh, J. Srebrny, C. Theisen, C. A. Ur, J. J. Valiente-Dobón, K. O. Zell, and M. Zielińska, Phys. Rev. Lett. **100**, 102502 (2008).
[11] E. A. McCutchan, C. J. Lister, T. Ahn, R. J. Casperson, A. Heinz, G. Ilie, J. Qian, E. Williams, R. Winkler, and V. Werner, Phys. Rev. C **83**, 024310 (2011).
[12] G. F. Bertsch, M. Girod, S. Hilaire, J.-P. Delaroche, H. Goutte, and S. Péru, Phys. Rev. Lett. **99**, 032502 (2007).
[13] N. Hinohara, T. Nakatsukasa, M. Matsuo, and K. Matsuyanagi, Phys. Rev. C **80**, 014305 (2009).
[14] N. Hinohara, K. Sato, T. Nakatsukasa, M. Matsuo, and K. Matsuyanagi, Phys. Rev. C **82**, 064313 (2010).
[15] K. Kaneko, T. Mizusaki, Y. Sun, and S. Tazaki, Phys. Rev. C **92**, 044331 (2015).

[16] A. Villari, G. Bollen, M. Ikegami, S. Lidia, R. Shane, Q. Zhao, D. Alt, D. Crisp, S. Krause, A. Lapierre, D. Morrissey, S. Nash, R. Rencsok, R. Ringle, S. Schwarz, C. Sumithrarachchi, and S. Williams, in *Proc. of International Particle Accelerator Conference (IPAC'16), Busan, Korea, May 8-13, 2016* (2016) pp. 1287–1290.

[17] A. Gade and B. M. Sherrill., Physica Scripta **91**, 053003 (2016).

[18] D. Morrissey, B. Sherrill, M. Steiner, A. Stolz, and I. Wiedenhoever, Nuclear Instruments and Methods in Physics Research Section B: Beam Interactions with Materials and Atoms **204**, 90 (2003).

[19] A. Lapierre, S. Schwarz, T. M. Baumann, K. Cooper, K. Kittimanapun, A. J. Rodriguez, C. Sumithrarachchi, S. J. Williams, W. Wittmer, D. Leitner, and G. Bollen, Review of Scientific Instruments **85**, 02B701 (2014).

[20] E. Lunderberg, J. Belarge, P. C. Bender, B. Bucher, D. Cline, B. Elman, A. Gade, S. N. Liddick, B. Longfellow, C. Prokop, D. Weisshaar, and C. Y. Wu, Nuclear Instruments and Methods in Physics Research A **885**, 30 (2018).

[21] W. Mueller, J. Church, T. Glasmacher, D. Gutknecht, G. Hackman, P. Hansen, Z. Hu, K. Miller, and P. Quirin, Nuclear Instruments and Methods in Physics Research Section A: Accelerators, Spectrometers, Detectors and Associated Equipment **466**, 492 (2001).

[22] P. C. Bender, `https://github.com/pcbend/GRUTinizer/`.

[23] R. Brun and F. Rademakers, Nucl. Instr. Meth. in Phys. Res. A **389**, 81 (1997).

[24] NNDC, "Evaluated Nuclear Structure Data File (ENSDF),".

[25] J. de Boer and J. Eichler, "The reorientation effect," in *Advances in Nuclear Physics: Volume 1*, edited by M. Baranger and E. Vogt (Springer US, Boston, MA, 1968) pp. 1–65.

[26] T. Czosnyka, D. Cline, and C. Y. Wu, Bulletins of the American Physical Society **28**, 745 (1983).

[27] J. H. Hamilton, A. V. Ramayya, W. T. Pinkston, R. M. Ronningen, G. Garcia-Bermudez, H. K. Carter, R. L. Robinson, H. J. Kim, and R. O. Sayer, Physical Review Letters **32**, 239 (1974).

[28] H. Orihara, M. Takahashi, K. Murakami, Y. Ishizaki, T. Suehiro, K. Miura, Y. Hiratate, and H. Yamaguchi, in *Inst. Nucl. Study, University of Tokyo Annual Report* (1977).

[29] M. H. Macfarlane and S. C. Pieper, in *Report No. ANL-76-11 Rev. 1, ANL Report* (1978).

[30] S. J. Freeman, J. P. Schiffer, A. C. C. Villari, J. A. Clark, C. Deibel, S. Gros, A. Heinz, D. Hirata, C. L. Jiang, B. P. Kay, A. Parikh, P. D. Parker, J. Qian, K. E. Rehm, X. D. Tang, V. Werner, and C. Wrede, Phys. Rev. C **75**, 051301 (2007).

[31] R. Palit, H. C. Jain, P. K. Joshi, J. A. Sheikh, and Y. Sun, Phys. Rev. C **63**, 024313 (2001).

[32] K. Nomura, R. Rodríguez-Guzmán, and L. M. Robledo, Phys. Rev. C **95**, 064310 (2017).

[33] `http://nuclei.mps.ohio-state.edu/content/tables/2+properties.txt`.

[34] K. Kumar, Physical Review Letters **28**, 249 (1972).

[35] D. Cline, Annual Review of Nuclear and Particle Science **36**, 681 (1986).

[36] J. Wood, E. Zganjar, C. D. Coster, and K. Heyde, Nuclear Physics A **651**, 323 (1999).

[37] M. Matsuo, T. Nakatsukasa, and K. Matsuyanagi, Progress of Theoretical Physics **103**, 959 (2000).

[38] K. Kaneko, T. Mizusaki, Y. Sun, and S. Tazaki, Physical Review C **89**, 011302(R) (2014).

[39] P.-G. Reinhard, D. J. Dean, W. Nazarewicz, J. Dobaczewski, J. A. Maruhn, and M. R. Strayer, Phys. Rev. C **60**, 014316 (1999).